



Effect of titanium addition on the microstructure, electrical conductivity and mechanical properties of copper by using SPS for the preparation of Cu-Ti alloys



Azunna Agwo Eze ^{a,*}, Tamba Jamiru ^a, Emmanuel Rotimi Sadiku ^b,
Mondiu Olayinka Durowaju ^{b,c}, Williams Kehinde Kupolati ^d, Idowu David Ibrahim ^a,
Babatunde Abiodun Obadele ^e, Peter Apata Olubambi ^e, Saliou Diouf ^{b,f}

^a Department of Mechanical Engineering, Mechatronics and Industrial Design, Tshwane University of Technology, South Africa

^b Institute of Nano Engineering Research (INER) and Department of Chemical, Metallurgical and Materials Engineering, Tshwane University of Technology, South Africa

^c Department of Mechanical Engineering, Ladoko Akintola University of Technology, Nigeria

^d Department of Civil Engineering, Tshwane University of Technology, South Africa

^e Department of Chemical Engineering, University of Johannesburg, South Africa

^f Department of Physics, Cheikh Anta Diop, University of Dakar, Senegal

ARTICLE INFO

Article history:

Received 26 September 2017

Received in revised form

8 November 2017

Accepted 10 November 2017

Available online 11 November 2017

Keywords:

Copper-titanium alloys

Electrical conductivity

Mechanical properties

ABSTRACT

This study assessed the electrical conductivity and the mechanical properties of pure Cu, 1 and 2.6 mass % Ti additions in a composition of CuTi0.014 and CuTi0.035 in region of Cu-solid solution, with the aim of studying the effect of titanium additions on the properties of copper. A sample of pure Cu, CuTi0.014 and CuTi0.035 were prepared in a plastic canister and mixed with alumina balls for 3 h at 49 rpm. The powdered samples were sintered at a temperature of 650 °C, with a punch load of 50 MPa, a dwelling time of 5 min and a heating rate of 50 °C/min. The results showed that the electrical conductivity of Cu, CuTi0.014 and CuTi0.035 are: 4.8, 5.0 and 4.2 (S/m) at temperatures of 345, 550 and 319 °C, respectively. The relative densities of the sintered samples are 96.76, 96.30 and 86.33% for Cu, CuTi0.014 and CuTi0.035, respectively. The Vickers hardness data of the sintered samples show that CuTi0.035 has the highest value (~749 MPa), followed by CuTi0.014 (~724 MPa) and pure Cu with (~645 MPa). In addition, the predicted yield strength (YS) and ultimate tensile strength (UTS) of the sintered samples were investigated. The YS are 1604, 1552 and 1395 MPa for CuTi0.035, CuTi0.014 and Cu, respectively. In similar other, the UTS are 1318, 1285 and 1182 MPa. The addition of 1 and 2.6 mass % Ti improved the corrosion resistivity of Cu in H₂SO₄ acid environment. Also, the addition of the 2.6 and mass % of Ti increases the coefficient of friction of Cu under dry sliding condition with a load of 25 N. The microstructures of the sintered CuTi0.014 and CuTi0.035 showed the precipitation of Ti. However, CuTi0.014 alloy has the best properties and is an ideal candidate for elevated temperature application. This composition of CuTi alloys can be used in the areas where Cu is required to maintain good electrical and mechanical properties at elevated temperatures (above room temperature) applications.

© 2017 Elsevier B.V. All rights reserved.

1. Introduction

Researches on copper-titanium alloys (Cu-Ti) have gained prevalent attention because of its properties, such as high strength, fine electrical conductivities, superior corrosion resistance, better antiseptic properties and a possible aspirant as a substitute for

costly and poisonous copper-beryllium alloys (Cu-Be). The aforementioned properties of copper-titanium alloys make it useful in heat transfer application [1], enhancement of the quality of silicon solar cells [2], electronic devices, such as connectors and relay controls [3] and biomedical appliances [4–7]. The exceptional electrical and mechanical properties of copper-titanium alloy have also encouraged investigations of interest in both basic metallurgy and realistic applications of the alloys [3,8–17]. Copper-titanium alloys have great promises in the industry as a replacement for

* Corresponding author.

E-mail addresses: ezeaaben@gmail.com, ezeaa@tut.ac.za (A.A. Eze).

copper-beryllium alloys. Copper-beryllium alloys have been extensively used as materials with superior electrical conductivity and excellent strength. However, these alloys (Cu-Be) have been reported to be costly and creates health risks, owing to the poisonous nature of beryllium when exposed to the atmosphere during processing, such as: melting, casting and hot working operation [18]. However, sizeable amounts of research works had been done in the investigation of the microstructure, mechanical properties and electrical conductivity of copper-titanium alloys, with the major aim of developing a replacement for the expensive and deadly copper-beryllium alloys for superior strength and standard conductivity application [1,9,12,19–28].

This study applies the spark plasma sintering (SPS) technique as a means of consolidation of the copper-titanium alloys. Minor work has been reported on the use of spark plasma sintering method, which has, lately, been established to be an efficient technique for the production of ceramic- and metallic-based composites. The benefits of spark plasma sintering over and above other production techniques include: rapid sintering, lower sintering temperatures, prevention of grain coarsening, avoidance of unnecessary reactions between the dissimilar phases, efficient sintering and fabrication of materials that are in close proximity to their net shape [29–33]. Without a doubt, there have been reports in the literature, on the spark plasma sintering of copper-titanium powder or its related alloys [34–39] as well as on the alloy electrical and thermal conductivities during spark plasma sintering [28,40–45]. It was, therefore, decided in this study, to investigate the spark plasma sintering behavior of copper-titanium powders and their electrical conductivities during sintering. Therefore, the attention in this study will be focused on investigating the effect of 1 and 2.6 mass % titanium additions at a sintering temperature of 650 °C on the: microstructure, mechanical properties and the electrical conductivities of copper.

2. Materials and method

The starting powders used in this study are copper (Cu) and titanium (Ti) of the same purity and particles sizes of 99.0% and $-44\ \mu\text{m}$, respectively, supplied by Alfa Aesar. Samples of copper containing 1 and 2.6 mass % of titanium in the composition of CuTi0.014 and CuTi0.035 powder were prepared and mixed in the region of Cu-solid solution. Pure copper and the two copper alloys powdered mixture were separately inserted in a plastic canister with alumina balls and mixed for three hours in Turbula shaker mixer apparatus for 49 rpm. The control sample (Cu), the CuTi0.014 and CuTi0.035 admixed powders were sintered at a temperature of 650 °C, with a punch load of 50 MPa, dwelling time of 5 min and a heating rate of 50 °C/min in a sintering system model HHPD 25 apparatus put on by FCT Germany, which was also used to determine the electrical conductivity against temperature of the powdered samples. The elemental composition of CuTi mixture are shown in Table 1, were mixed by using the T2F Turbula shaker, inside a dry environment, for a period of 3 h at a stable rotational speed of 49 rpm at room temperature.

Table 1
Elemental composition of CuTi mixture.

Samples Identity	Composition of pure Cu and CuTi alloys	
	Copper (Cu)	Titanium (Ti)
Pure Copper (Cu)	100	–
CuTi0.014	98	2 = 1 mass %
CuTi0.035	95	5 = 2.6 mass %

2.1. Electrical and thermal conductivity of the powders during sintering

For the electrical conductivity as a function of temperature test, one portion of Cu and the blended powdered alloys of 1 and 2.6 mass % titanium additions (CuTi0.014 and CuTi0.035) were put inside the non-conductive (Si_3N_3) die of diameter and height of 20 and 2 mm, respectively and were connected with a copper-based molybdenum punch. The creation of electrical contact between the powders tested in the die and punch was made possible through an applied compressive load of 10 KN. An electrical power of 8 KW was used, as the temperature stabilized, the 2 KW of electrical power was applied at an interval of 2 min. The tests were stopped at a temperature where the electrical conductivity of the samples was at the maximum before the powders tested started sintering; this is to know the maximum temperature at which maximum electrical conductivity can be attained by the tested powders before sintered. A spark plasma sintering (SPS) apparatus HHPD25 was used for the electrical conductivity test on (and full sintering of) the copper, blended powdered alloys of 1 and 2.6 mass % titanium additions (Cu, CuTi0.014 and CuTi0.035 respectively) at a temperature of 650 °C.

2.2. Mechanical properties of full spark plasma sintering Cu, CuTi0.014 and CuTi0.035 alloys

Another portion of the Cu, CuTi0.014 and CuTi0.035 were consolidated by using spark plasma sintering technique at a heating rate of 50 °C/min, dwelling time of 5 min, compressive load of 50 MPa and a sintering temperature of 650 °C. The morphology of the powders and the sintered samples were studied by using the Field Emission Scanning Electron Microscopy (JEOL, JSM-7600f), which was incorporated with an energy dispersive x-ray spectrometer (EDS) detector. Prior to scanning electron microscopy (SEM) analysis, the sintered samples were grinded and polished to mirror surface. The densities and relative densities of the sintered sample were determined and the micro-hardness was measured by using the Vickers indentation method at an applied load of 100 g force with a time of 15 s. The Vickers hardness (HV) results, in MPa, were used in equations (1) and (2) to obtain the predicted yield strength (YS) and ultimate tensile strength (UTS) of the sintered samples. According to Hashemi [46], the minimum and maximum error, in %, between the measured yield strength (YS) and the predicted value (equation (1)) was 0.2 and 13.8 MPa, respectively. In this study, equations (1) and (2) were used to compute the YS and UTS [46].

$$YS = 2 \times HV + 105 \quad (1)$$

$$UTS = 1.3 \times HV + 344 \quad (2)$$

2.3. Corrosion and wear test

Corrosion tests were conducted on the fully sintered samples. Electrochemical studies were therefore carried out in 1 mol of sulphuric acid (H_2SO_4) solution environment that contained the solid sintered samples (working electrode), a counter electrode, which was made-up of graphite and saturated silver/silver chloride, which served as the reference electrode. The corrosion tests were carried out with VersaSTAT four, with versa studio four software. Potentiodynamic polarization method was used to review the general electrochemical behavior of the sintered Cu and alloys containing 1 and 2.6 mass % titanium additions (Cu, CuTi0.014 and CuTi0.035). Before the scanning, all the tested samples were

immersed in the electrolyte for 5 min to enable them to stabilize before the open circuit potential measurement, which lasted for about two hours. All the samples tested were scanned at a scan rate of 2 mV/s with potential ranging from 0.5 to 1.5 V.

Tribological behavior of the sintered Cu and alloys containing 1 and 2.6 mass % titanium addition (Cu, CuTi0.014 and CuTi0.035), in a reciprocating dry sliding condition, was conducted by using a CETR-2-UMT tribometer, provided with a computer-controlled ball-on-disc arrangement that operated at room temperature. A 10 mm diameter counter surface ball, made of tungsten carbide (WC) was used to slide against the tested samples in a reciprocating motion, under a load of 25 N and at a frequency of 5 Hz. A perpendicularly downwards load was applied on the samples tested, with a motor-driven moving parts that utilize a load measuring device for the response in order to sustain a stable applied load. The coefficient of friction (μ) was constantly recorded during the sliding operation and the results were obtained from the UMT-2-CETR apparatus software.

3. Results and discussion

3.1. Microstructure image analysis of as-received powders

The morphology of the as-received powders was observed with a field emission scanning electron microscopy, which was fitted with energy dispersive x-ray spectrometer. Fig. 1a and b shows the scanned electron microscopy (SEM) surface morphology of the two as-received powders. The copper powder particles have very small size/shape of large agglomerates, while the titanium powdered particles have large and irregular shapes.

3.2. Electrical conductivity of Cu, Cu-2Ti and Cu-5Ti powdered alloys

In Fig. 2, each sample tested was stopped at a point where the electrical conductivity ceased to increase with temperature. Fig. 2 shows the variation of Cu, alloys of CuTi0.014 and CuTi0.035 powders as functions of temperature. It can be seen that the electrical conductivity of pure Cu increases with temperature to a maximum value of 4.8 (S/m) at a temperature of 345 °C, as shown in Fig. 2 and Table 2. Explanation of the event that resulted in a decrease in electrical conductivity of copper beyond 345 °C, could be the apparent introduction of phonons, which is the ideal resistivity of the materials [47]. In pure metals, phonons are accountable for the dispersing of electrons by the pulsating lattice ion of the metal due to high thermal energy absorbed in the atom.

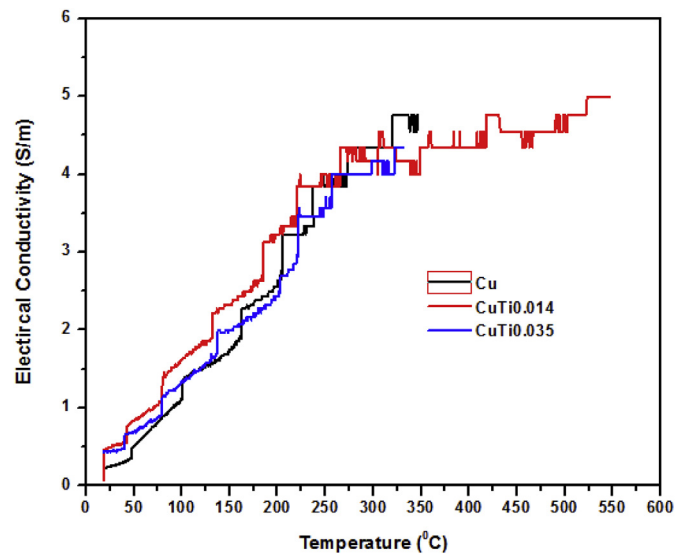


Fig. 2. Electrical conductivity versus Temperature (°C) of Cu, CuTi0.014 and CuTi0.035 alloys.

When temperature increases in the metal, thermal energy will be induced and this will cause the ion to shift from their stable position, thereby, obstructing the free moving electrons. At low temperature, phonon is insignificant because the ions remained in their stable location in the lattice of the atoms. However, metals can conduct electricity as long as their ions remained stable in their lattice without being disruptive of the free movement of the electrons, which are charged carriers [47]. The addition of 2.6 mass % titanium (CuTi0.035) showed an increase in electrical conductivity with temperature, to a maximum value of 4.2 (S/m) at a temperature of 319 °C, which was lower when compared to Cu and CuTi0.014. The addition of 1 mass % titanium (CuTi0.014) showed better improvement in the electrical conductivity of Cu at elevated temperature, which was at a maximum value of 5.0 (S/m). The poor electrical conductivity observed in the CuTi0.035 alloy can be attributed to the high concentration of Ti addition that could have increased the resistivity of the alloy. This electrical conductivity behavior observed in CuTi0.035 alloy was in line with the work of Nagarjuna et al. [42], which stated that Ti addition up to about 4.0 wt % increased the resistivity of Cu. The electrical conductivity observed in CuTi0.014 alloy is attributed to the low concentration of Ti in the alloy, which acted as heat absorber as the temperature

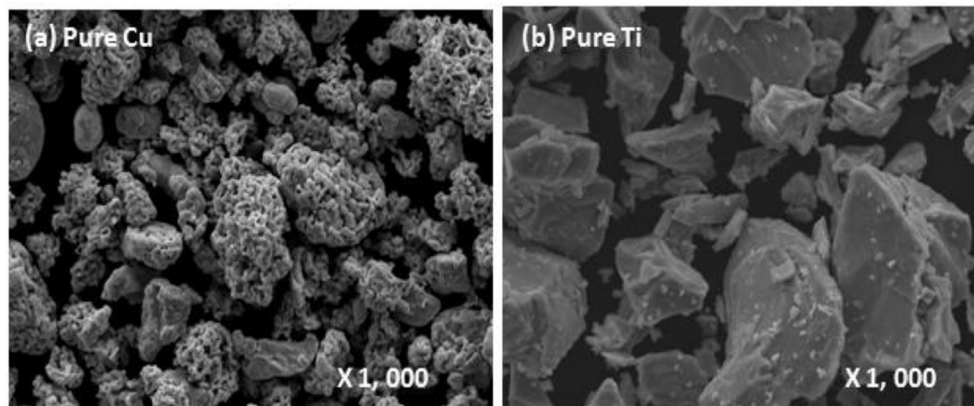


Fig. 1. Scanning Electron Microscopy image showing morphology of as-received Cu and Ti at the same magnification: $\times 1,000$.

Table 2

The electrical conductivity values attained with temperature of Cu and the alloys of 1 and 2.6 mass % Ti additions.

Samples composition	Electrical conductivity (S/m)	Temperature at highest electrical conductivity (°C)	Temperature in Kelvin (K)
Cu	4.8	345	618.15
CuTi0.014	5.0	550	823.15
CuTi0.035	4.2	319	592.15

increases. These phenomena are considered to result from decreases in the amount of the dissolved Ti by precipitation [28], in the CuTi0.014 alloy. The continuous electrical conductivity at elevated temperature observed on CuTi0.014 alloy can also be that the precipitated Ti particle was absorbing excess heat that could have disrupted the lattice of the copper atoms, thereby maintaining the smooth movement of the electrons in the entire CuTi0.014 alloy. On the other hand, the improvement in the electrical conductivity observed, following the addition of 1 mass % Ti addition can also be attributed to the presence of Ti particles as an impurity, which can reduce the resistivity of copper in the CuTi0.014 alloy. Many research works [30,47–50] had shown that the presence of impurities lowers the electrical resistivity of metals, hence, the improvement in its electrical conductivity.

3.3. Displacement and displacement rate with temperature of the powders during SPS

In this study, the particles sizes and the sintering parameters remained constant for the samples tested. After the electrical conductivity test, which was stopped before the full sintering of the samples began; another portion of the same powdered mixture was fully sintered at a sintering temperature of 650 °C, with a compressive load of 50 MPa, a dwelling time of 5 min and a heating rate of 50 °C/min on the SPS apparatus. Figs. 3 and 4 showed typical spark plasma sintering densification and densification rate as functions of temperature curves for: Cu, CuTi0.014 and CuTi0.035 alloys. This explains the punch compressive displacement against increased in temperature as the powdered particles were being sintered. In Fig. 3, it can be seen that the densification of Cu powders was observed to have started at 550 °C and reaches a

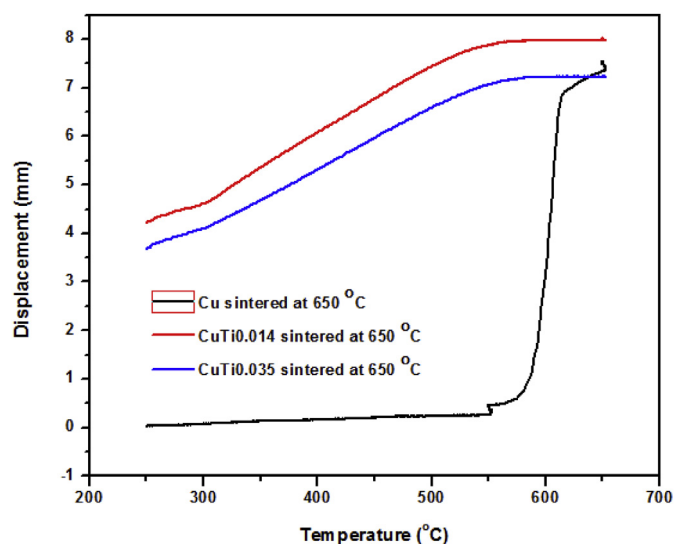


Fig. 3. Spark plasma sintering densification versus temperature curves of Cu, CuTi0.014 and CuTi0.035 alloys at 650 °C.

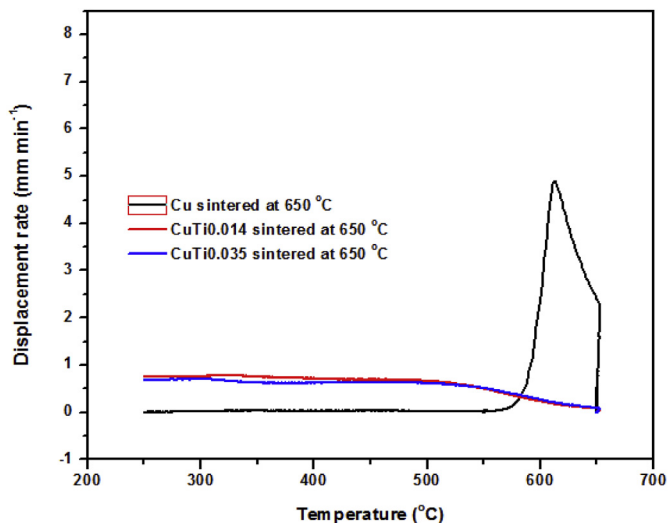


Fig. 4. Spark plasma sintering densification rate versus temperature curves of Cu, CuTi0.014 and CuTi0.035 alloys at 650 °C.

maximum densification rate of 600 °C. However, densification was improved with increased temperature (i.e. between 550 and 600 °C). The densification of CuTi0.014 and CuTi0.035 alloys was observed to have a proportional increase in the displacement of the particle with a temperature that began from 250 °C and reaching a maximum at 500 °C. It is important to know that sample densification was already completed on reaching the dwelling temperature of 650 °C. However, there was no observed shrinkage of the particles outside the temperature slope. The densification of the powdered particles as a function of temperature curve in CuTi0.014 was observed to be of the same shape, but slightly above that of CuTi0.035 alloy. The densification of particles with temperature curve of the two alloys was seen to be above (and of different shape when compared with) that of pure Cu. These differences can be attributed to the presence of Ti particles in the matrix of Cu, which seems to have reduced the densification temperature of Cu.

3.4. Relative density, porosity, microhardness, yield strength and ultimate tensile strength of the sintered Cu, CuTi0.014 and CuTi0.035

The results for the relative density, porosity, micro-hardness, calculated yield strength and ultimate tensile strength of Cu, CuTi0.014 and CuTi0.035 alloys are summarized in Table 3. The theoretical density (TD) used in this study was obtained using equation (3) and the final relative density was obtained using Archimedes's method. The porosity of the sintered samples was determined by using equation (4) [51].

$$\text{Theoretical density (TD)} = 1 \div \left(\frac{\text{wt.\% of sample A}}{\text{density of sample A}} + \frac{\text{wt.\% of sample B}}{\text{density of sample B}} \right) \quad (3)$$

$$P = 1 - \left(\frac{ED}{TD} \right) \times 100 \quad (4)$$

where P = Porosity, ED = Experimental density and TD = Theoretical density.

At a sintering temperature of 650 °C and a compressive load of 50 MPa, heating rate of 50 °C/min and a holding time of 5 min, the experimental density, relative density and porosity of the sintered

Table 3
Summary of samples properties.

Sample composition	Compositions (Vol. %)		T D (g/cm ³)	SPS (°C)	ED (g/cm ³)	RD (%)	P (%)	MH (MPa)	PYS (MPa)	PUTS (MPa)
	Cu	Ti								
Cu	100	—	8.96	650	8.68	96.76	3.13	644.91	1394.82	1182.38
CuTi0.014	98	2 = 1 mass %	8.87	650	8.60	96.30	3.04	723.66	1552.32	1284.76
CuTi0.035	95	5 = 2.6 mass %	8.70	650	8.38	86.33	3.68	749.35	1603.70	1318.16

Theoretical density (TD), spark plasma sintering (SPS) temperature, experimental density (ED), relative density (RD), porosity (P), micro-hardness (MH), predicted yield strength (PYS) and the predicted ultimate tensile strength (PUTS).

samples were recorded as follows: for pure Cu density was 8.68 g/cm³, relative density was 96.76% and porosity was 3.10%; while CuTi0.014 alloy density was 8.60 g/cm³, relative density was 96.30% and porosity was 3.04% and CuTi0.035 alloy density was 8.38 g/cm³, relative density was 86.33% and porosity was 3.68%. However, the higher density and relative density observed in pure Cu over its alloys is attributed to good densification observed, as shown in Fig. 5, which gradually increased with temperature from the onset and rapidly appreciated at a temperature of 550 °C to a maximum at 600 °C (Figs. 3 and 4). The CuTi0.014 alloy is observed to have the lowest porosity, but with relative density value that is lower than that of pure Cu, as observed in Table 3. The lower porosity observed is a sign of good densification and the even dispersion of titanium particles all over the matrix of Cu, as the particles of Ti started to precipitate to occupy the voids. The result observed is presented in Fig. 6. In addition, the relative density that was lower when compared to that of pure Cu can be as a result of the presence of Ti, since Ti is known to have lower density when compared to Cu, which brought about the reduction in the density of Cu, observed in the alloy. CuTi0.035 alloy was observed to have the lowest experimental density, relative density and highest porosity when compared to pure Cu and CuTi0.014 alloy. This shows that the particles of titanium in the alloy were not evenly dispersed in the matrix of Cu. Therefore, full densification may not be achieved, since some large, irregular and un-deformed particles of titanium can be seen in Fig. 7, which is believed to be responsible for the low

density, relative density and higher porosity observed the CuTi0.035 alloy. It was observed that as the percentage of Ti addition increased from 1 to 2.6 mass % in the Cu-Ti alloys, the density and relative density of Cu reduced. It can be noted that the density, relative density and porosity values for pure Cu obtained, in this study, were similar to that obtained by Sule et al. [51]. In their work, pure Cu was sintered at a temperature of 820 °C and compressive load of 30 MPa and they obtained a density of 8.69 g/cm³, with a relative density of 97.20% and porosity of 2.8%. The little disparity in density, relative density and porosity values of pure Cu between their work and the current study is attributed to the differences in consolidation parameters. Table 3 also shows the values of the micro-hardness, calculated yield strength and the ultimate tensile strength of Cu, CuTi0.014 and CuTi0.035 alloys. The hardness values obtained are evidence of the densification after sintering and the homogeneity of the reinforcing materials [30]. CuTi0.035 alloy records the highest hardness value; followed by CuTi0.014 alloy, while pure Cu records the lowest value. The addition of titanium particles increased the hardness value of Cu, which may be attributed to precipitate of Ti in the Cu-Ti alloys. When the titanium concentration is very high, the wettability in Cu-Ti alloys will improve remarkably because of the continuous thin layer that is formed at the interface at the initial stage of the reaction with Cu [52]. However, according to Wolf et al. [53], the maximum strength is obtained when the reaction layer is very thin. It was reported by Nagrajuna et al. [54] that the hardness and yield strength in the

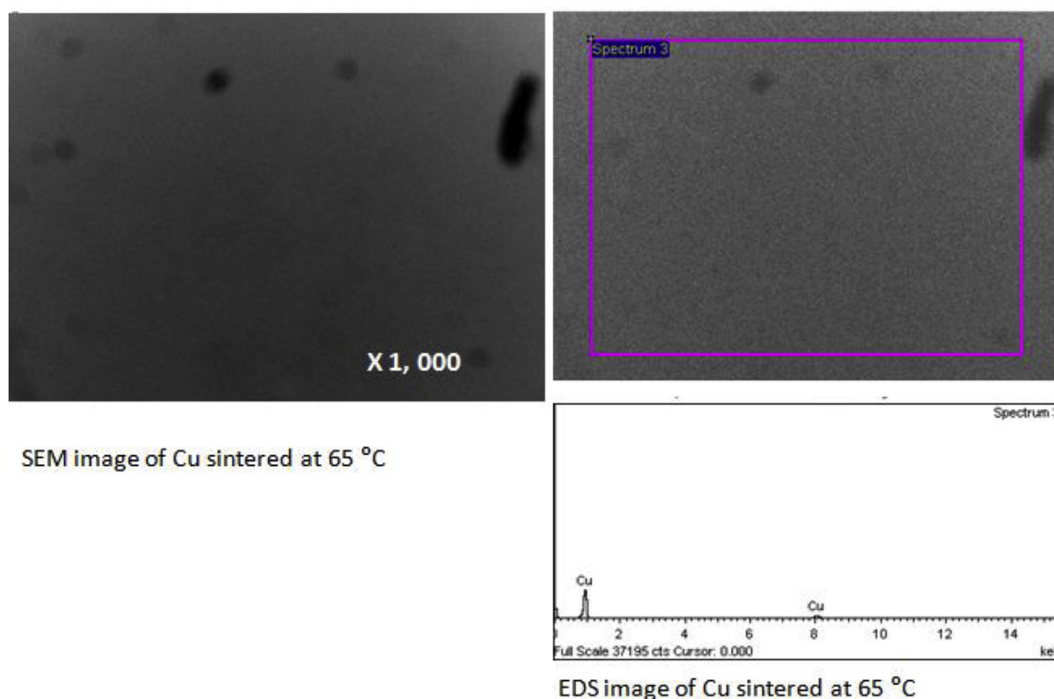


Fig. 5. SEM and EDS images of the sintered Cu at 650 °C.

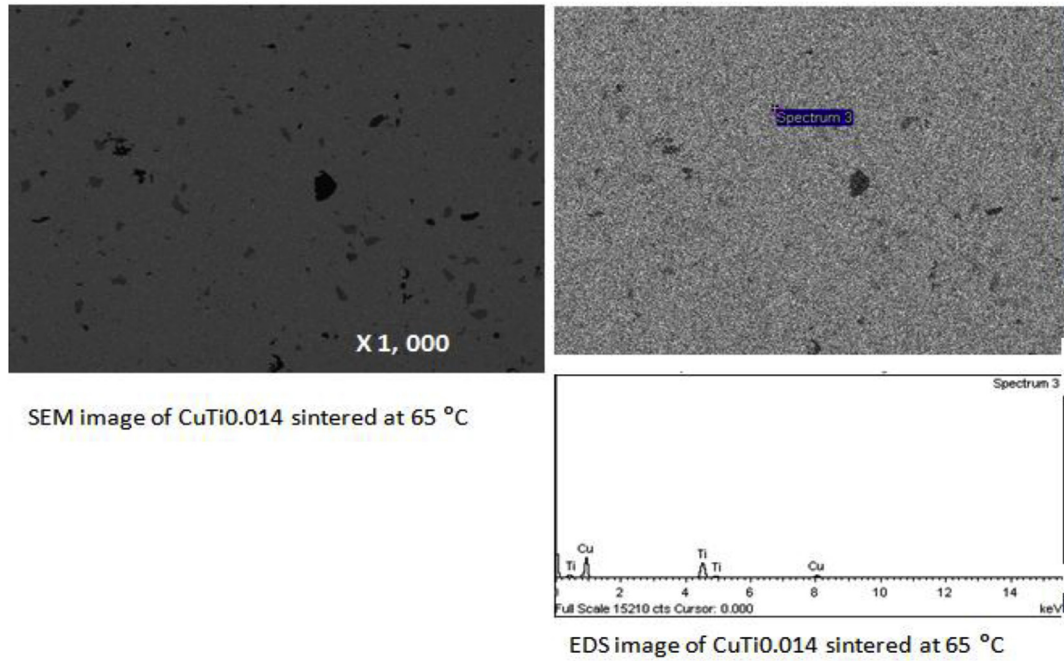


Fig. 6. SEM and EDS images of the sintered CuTi0.014 at 650 °C.

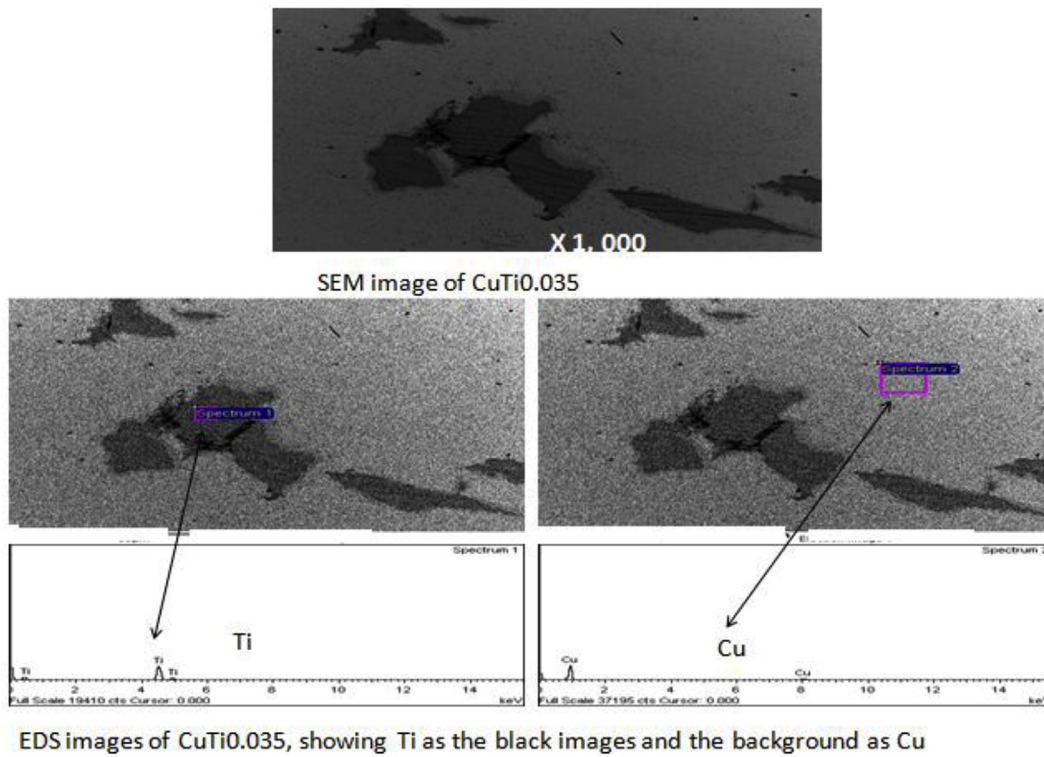


Fig. 7. SEM and EDS images of the sintered CuTi0.035 at 650 °C.

solution treated copper-titanium alloys increased linearly, up to about 4.0 wt % Ti, beyond which a quick increase was examined with the extra addition of titanium. The yield strength and ultimate tensile strength have a direct relationship with the hardness, as represented in Equations (1) and (2). CuTi0.035 alloy still recorded the highest yield strength and ultimate tensile strength.

3.5. Microstructural and EDS images analysis of the sintered samples

Figs. 5–7 show the SEM images and EDS analysis of pure Cu, CuTi0.014 and CuTi0.035 alloys sintered at 650 °C. In Fig. 5, it can be seen that there was an even distribution of Cu particles all over the

sintered sample. The EDS graph confirms that there was no contamination during the sintering process. This explains why it recorded the highest density and relative density. Fig. 6 shows the SEM and EDS of CuTi0.014 alloy, having distributed particles of Ti (black pigments). This signifies good densification, which is responsible for the alloy to have lower porosity value when compared to other samples, while in Fig. 7, lumps of irregular and un-deformed Ti particles were observed. This shows poor densification, which resulted in the high porosity, lower density and relative density that were recorded, as stated earlier.

3.6. Corrosion studies of the sintered samples at 650 °C

Figs. 8 and 9 and Table 4 show the effect of the 1 and 2.6 mass % titanium additions on the uniform corrosion behavior of pure Cu. Typical open circuit potential (OCP) curves for sintered Cu and alloys, presented in Fig. 8, revealed that Cu and alloys containing 2.6 mass % titanium were comparatively stabilized with time when compared with the alloy containing 1 mass % titanium, which was not stable from the onset. The stability in the potentials at 0.00 V of pure Cu and the alloy containing 2.6 mass % titanium additions specifies that both were thermodynamically stable with time in a sulphuric (H_2SO_4) acid solution environment. From the same results, the potentials of the alloy containing 1 mass % titanium additions, started from -0.12 V and progressed to a negative potential of about -0.01 V, where it became relatively stabilized with increased in exposure time, with this stability occurring in the neighborhood of pure Cu. The more alloy containing 1 mass % titanium additions, the more the move towards the direction of positive potentials, suggesting that CuTi0.014 alloy has a higher tendency to resist corrosion as time progresses, by the formation of a passive film of likely titanium oxide.

The characteristic polarization curve presented in Fig. 9 reveals only a slight difference in the corrosion potentials of Cu, alloys containing 2.6 and 1 mass % titanium addition. Furthermore, from the OCP results, the potentials of the alloy containing 2.6 mass % titanium addition was lower than that of Cu from the onset, but after a period of 710 s, it, however, recorded a stabilized effect, with a higher dissolution potential above others and in contrast from the polarization result, where it recorded the lowest corrosion current density value when compared to others. While the alloy containing 1 mass % titanium addition was observed to had a dissolution

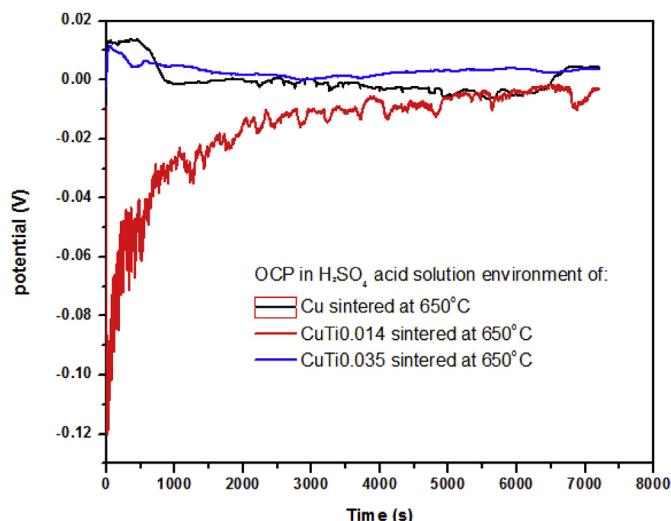


Fig. 8. OCP in H_2SO_4 acid solution environments of Cu, CuTi0.014 and CuTi0.035.

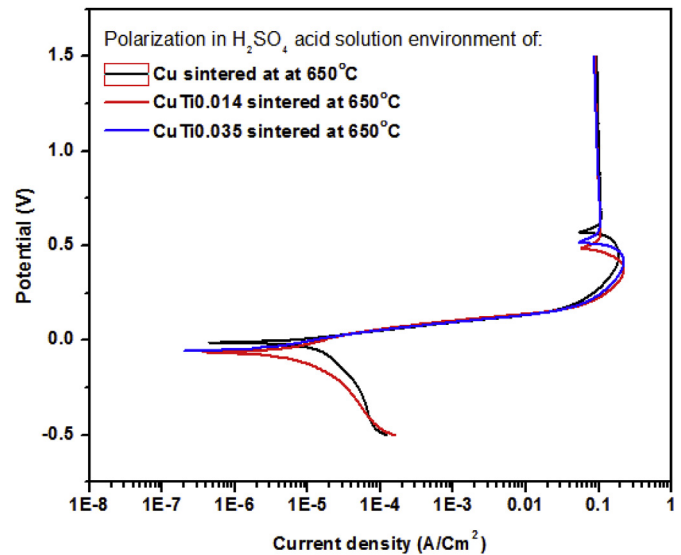


Fig. 9. Polarization in H_2SO_4 acid solution environments of: Cu, CuTi0.014 and CuTi0.035.

Table 4

Corrosion properties of: Cu, CuTi0.014 and CuTi0.035 alloys sintered at 650 °C.

Composition (vol. %)	E_{corr} (V)	I_{corr} (A/cm ²)	Corrosion rate (mm/y)
Cu	-0.01	$1.635E^{-6}$	$1.895E^{-2}$
CuTi0.014	-0.06	$1.609E^{-6}$	$1.826E^{-2}$
CuTi0.035	-0.05	$9.157E^{-7}$	$1.005E^{-2}$

potential that was closely similar to that of pure Cu, as time progressed, as earlier predicted from the OCP results, but was found to have the highest corrosion current density value, as observed in the polarization results. An explanation to this behavior of alloy containing 1 mass % titanium addition can possibly be as a result of a number of heterogeneities in the alloy, through sintering at a temperature of 650 °C, which could have caused the fading-away of titanium and leaving more Cu in the matrix of the alloy with an increase in the exposure time.

3.7. Coefficient of friction under dry sliding condition of the sintered: Cu, Cu-2Ti and Cu-5Ti alloys

After spark plasma sintering of the samples at a temperature of 650 °C, the wear behavior of the sintered samples was tested. A 10 mm diameter counter surface ball, made of tungsten carbide (WC) was used to slide against the samples tested, in a reciprocating motion, under a load of 25 N and at a frequency of 5 Hz. Fig. 10 shows the variation of the coefficient of friction as a function of the sliding time for: pure Cu, CuTi0.014 and CuTi0.035 alloys under dry sliding conditions mentioned above. As it can be seen, the coefficient of friction of Cu is the least of the 3 different samples tested; it started from 0.12 to 0.37. CuTi0.014 alloy recorded lower coefficient of friction after that of Cu (when compared with CuTi0.035 alloy), which started from 0.15 to 0.41. From this point onwards, it maintained a steady-state wear. While CuTi0.035 alloy recorded the highest coefficient of friction, which at the initial stage, under the applied load, started to wear from 0.14 to 0.43, where it became steady as the time progressed. Generally, the curves show that as the concentration of titanium addition increases from 1 to 2.6 mass %, the higher the coefficient of friction of Cu recorded. This can be attributed to the poor tribological

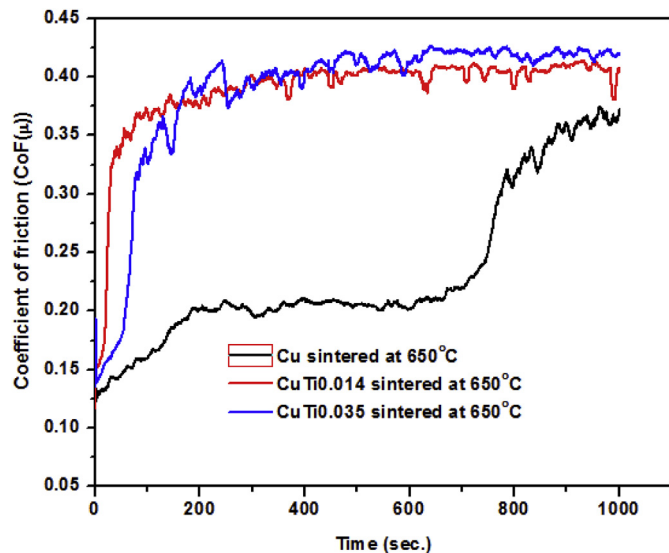


Fig. 10. Coefficient of friction under dry sliding condition of sintered: Cu, CuTi0.014 and CuTi0.035 alloys.

characteristics of titanium, which has been confirmed by other researchers [5,55,56].

4. Conclusion

In this study, it has been shown that the alloy of 1 mass % Ti (CuTi0.014) addition increases the electrical conductivities of Cu at elevated temperatures. The 2.6 mass % Ti (CuTi0.035) additions improved the corrosion resistivity of Cu in a H_2SO_4 acid solution environment. However, the 1 and 2.6 mass % Ti addition increased the micro-hardness, thermal conductivity, yield strength and ultimate tensile strength of Cu. The presence of 1 and 2.6 mass % Ti also altered the microstructures of Cu. It was also observed that the addition of 1 and 2.6 mass % Ti increased the coefficient of friction of Cu under dry sliding conditions. With these findings, it is envisaged that CuTi alloys can be used in the area where Cu is required to maintain good electrical and mechanical properties at elevated temperatures (above room temperature) applications, and also find applications in an acid environment, without any significant acidic attack on the materials.

Acknowledgements

The authors, Eze AA and ID Ibrahim, gratefully acknowledge the Council of Scientific and Industrial Research (CSIR) and the Department of Science and Technology (DST), South Africa, for providing the financial support for this research.

References

- [1] S. Nagarjuna, Thermal conductivity of Cu-4.5 Ti alloy, *Bull. Mater. Sci.* 27 (2004) 69–71.
- [2] F. Dehghan Nayeri, B. Esfandiarpour, A. Behnam, M.H. Maleki, Ohmic contact of Cu/Mo and Cu/Ti thin layers on multi-crystalline silicon substrates, *Iran. J. Chem. Chem. Eng. (Int. Engl. Ed.)* 26 (2007).
- [3] S. Semboshi, E. Hinamoto, A. Iwase, Age-hardening behavior of a single-crystal Cu–Ti alloy, *Mater. Lett.* 131 (2014) 90–93.
- [4] M. Kikuchi, Y. Takada, S. Kiyosue, M. Yoda, M. Woldu, Z. Cai, et al., Mechanical properties and microstructures of cast Ti–Cu alloys, *Dent. Mater.* 19 (2003) 174–181.
- [5] C. Ohkubo, I. Shimura, T. Aoki, S. Hanatani, T. Hosoi, M. Hattori, et al., Wear resistance of experimental Ti–Cu alloys, *Biomaterials* 24 (2003) 3377–3381.
- [6] L. Tsao, Basic electrochemical behavior of Ti-7Cu alloys for medical applications, *Acta Phys. Polonica-Series A General Phys.* 122 (2012) 561.

- [7] L. Tsao, Effects of Cu addition on the microstructure and mechanical properties of Ti15Sn alloys, *Mater. Sci. Eng.* 698 (2017) 98–103.
- [8] J. Cornie, A. Datta, W. Soffa, An electron microscopy study of precipitation in Cu–Ti sideband alloys, *Metall. Trans.* 4 (1973) 727–733.
- [9] A. Datta, W. Soffa, The structure and properties of age hardened Cu–Ti alloys, *Acta Metall.* 24 (1976) 987–1001.
- [10] R. Ecob, J. Bee, B. Ralph, The structure of the β -phase in dilute copper–titanium alloys, *Phys. Status Solidi(a)* 52 (1979) 201–210.
- [11] R. Ecob, J. Bee, B. Ralph, The cellular reaction in dilute copper–titanium alloys, *Metall. Mater. Trans.* 11 (1980) 1407–1414.
- [12] D.E. Laughlin, J.W. Cahn, Spinodal decomposition in age hardening copper–titanium alloys, *Acta Metall.* 23 (1975) 329–339.
- [13] S. Nagarjuna, M. Srinivas, K. Balasubramanian, D. Sarma, The alloy content and grain size dependence of flow stress in Cu Ti alloys, *Acta Mater.* 44 (1996) 2285–2293.
- [14] L. Nesbit, D. Laughlin, Ordering in an off-stoichiometric Ni–Mo alloy, *Acta Metall.* 26 (1978) 815–825.
- [15] S. Semboshi, S. Sato, M. Ishikuro, K. Wagatsuma, A. Iwase, T. Takasugi, Investigation of precipitation behavior in age-hardenable Cu–Ti alloys by an extraction-based approach, *Metall. Mater. Trans. A* 45 (2014) 3401–3411.
- [16] W. Soffa, D. Laughlin, High-strength age hardening copper–titanium alloys: redivivus, *Prog. Mater. Sci.* 49 (2004) 347–366.
- [17] A.W. Thompson, J.C. Williams, Age hardening in Cu–2.5 wt pct Ti, *Metall. Mater. Trans.* 15 (1984) 931–937.
- [18] S. Nagarjuna, M. Srinivas, K. Balasubramanian, D. Sarma, Influence of polycrystalline grain size on yield and flow stress in Cu–1.5 wt% Ti alloy, *Scripta Metall. Mater.* 30 (1994) 1593–1597.
- [19] J. Dutkiewicz, Electron microscope study of the effect of deformation on precipitation and recrystallization in copper–titanium alloys, *Metall. Trans. A* 8 (1977) 751–761.
- [20] N. Grant, A. Lee, M. Lou, High Conductivity Copper and Aluminum Alloys, American Institute of Mining, Metallurgical, and Petroleum Engineers, Inc, New York, 1984, p. 103.
- [21] R. Knights, P. Wilkes, The precipitation of titanium in copper and copper–nickel base alloys, *Acta Metall.* 21 (1973) 1503–1514.
- [22] H. Michels, I. Cadoff, E. Levine, Precipitation-hardening in Cu–3.6 wt PCT Ti, *Metall. Trans.* 3 (1972) 667–674.
- [23] S. Nagarjuna, K. Balasubramanian, D.S. S, Effects of cold work on precipitation hardening of Cu–4.5 mass% Ti alloy, *Mater. Trans., JIM* 36 (1995) 1058–1066.
- [24] S. Nagarjuna, M. Srinivas, K. Balasubramanian, D. Sarma, Effect of alloying content on high cycle fatigue behaviour of Cu Ti alloys, *Int. J. Fatig.* 19 (1997) 51–57.
- [25] M. Saarivirta, High conductivity copper alloys—parts i–iii, *Met Ind* 103 (1963) 685–688.
- [26] M. Saarivirta, H. Cannon, Copper–titanium alloys, *Metal Progress* 76 (1959) 81–84.
- [27] S. Saji, E. Hornbogen, Combined recrystallization and precipitation reactions in a Cu–4 wt. percent ti-alloy, *Z Metallkd* 69 (1978) 741–746.
- [28] S. Suzuki, K. Hirabayashi, H. Shibata, K. Mimura, M. Isshiki, Y. Waseda, Electrical and thermal conductivities in quenched and aged high-purity Cu–Ti alloys, *Scripta Mater.* 48 (2003) 431–435.
- [29] A. Bellosi, F. Monteverde, D. Sciti, Fast densification of ultra-high-temperature ceramics by spark plasma sintering, *Int. J. Appl. Ceram. Technol.* 3 (2006) 32–40.
- [30] M. Durowoju, E. Sadiqu, S. Diouf, M. Shongwe, P. Olubambi, Spark plasma sintering of graphite–aluminum powder reinforced with SiC/Si particles, *Powder Technol.* 284 (2015) 504–513.
- [31] T. Hungria, J. Galy, A. Castro, Spark plasma sintering as a useful technique to the nanostructuring of piezo-ferroelectric materials, *Adv. Eng. Mater.* 11 (2009) 615–631.
- [32] N. Saheb, Z. Iqbal, A. Khalil, A.S. Hakeem, N. Al Aqeeli, T. Laoui, et al., Spark plasma sintering of metals and metal matrix nanocomposites: a review, *J. Nanomater.* 2012 (2012) 18.
- [33] F. Zhang, M. Reich, O. Kessler, E. Burkel, The potential of rapid cooling spark plasma sintering for metallic materials, *Mater. Today* 16 (2013) 192–197.
- [34] M. Antadze, R. Chedia, O. Tsagareishvili, A. Mikeladze, A. Gacheciladze, B. Margiev, et al., Metal-ceramics based on nanostructured boron carbide, *Solid State Sci.* 14 (2012) 1725–1728.
- [35] Q. Che, J. Zhang, X. Chen, Y. Ji, Y. Li, L. Wang, et al., Spark plasma sintering of titanium-coated diamond and copper–titanium powder to enhance thermal conductivity of diamond/copper composites, *Mater. Sci. Semicond. Process.* 33 (2015) 67–75.
- [36] H. Imai, K. Kondoh, S. Li, J. Umeda, B. Fugetsu, M. Takahashi, Microstructural and electrical properties of copper–titanium alloy dispersed with carbon nanotubes via powder metallurgy process, *Mater. Trans.* 55 (2014) 522–527.
- [37] H. Imaia, K.-Y. Chen, K. Kondoh, H.-Y. Tsai, Effect of alloying elements on mechanical properties and electrical conductivity of p/m copper alloys dispersed with vapor-grown carbon fiber, *Process. Properties Adv. Ceramics Comp. VII: Ceram. Trans.* 252 (2015) 383.
- [38] J. Li, H. Zhang, L. Wang, Z. Che, Y. Zhang, J. Wang, et al., Optimized thermal properties in diamond particles reinforced copper–titanium matrix composites produced by gas pressure infiltration, *Compos. Appl. Sci. Manuf.* 91 (2016) 189–194.
- [39] L. Xiyu, Y. Fenghuan, T. Yiqin, G. Yiping, P. Sianqi, Electric spark sintering technique and its applications, *Powder Metall. Technol.* 3 (1992) 003.

- [40] J. Lloyd, E. Neubauer, J. Barcena, W. Clegg, Effect of titanium on copper–titanium/carbon nanofibre composite materials, *Compos. Sci. Technol.* 70 (2010) 2284–2289.
- [41] J. Murray, The Cu–Ti (Copper–Titanium) system, *J. Phase Equil.* 4 (1983) 81–95.
- [42] S. Nagarjuna, K. Balasubramanian, D. Sarma, Effect of Ti additions on the electrical resistivity of copper, *Mater. Sci. Eng.* 225 (1997) 118–124.
- [43] T. Oku, A. Kurumada, T. Sogabe, T. Oku, T. Hiraoka, K. Kuroda, Effects of titanium impregnation on the thermal conductivity of carbon/copper composite materials, *J. Nucl. Mater.* 257 (1998) 59–66.
- [44] S. Semboshi, T. Al-Kassab, R. Gemma, R. Kirchheim, Microstructural evolution of Cu-1at% Ti alloy aged in a hydrogen atmosphere and its relation with the electrical conductivity, *Ultramicroscopy* 109 (2009) 593–598.
- [45] X. Yang, Y.-Q. Song, C.-G. Lin, C. Shun, Z.-Z. Fang, Effect of carbide formers on microstructure and thermal conductivity of diamond–Cu composites for heat sink materials, *Trans. Nonferrous Metals Soc. China* 19 (2009) 1161–1166.
- [46] S. Hashemi, Strength–hardness statistical correlation in API X65 steel, *Mater. Sci. Eng.* 528 (2011) 1648–1655.
- [47] A.A. Eze, Production of Binary Copper–titanium and Copper–niobium Alloys for Trolley Wire Applications Using Spark Plasma Sintering Techniques Spark Plasma Sintering Techniques, Masters dissertation, Tshwane University of Technology Pretoria, South Africa, 2016.
- [48] A. Eze, T. Jamiru, E. Sadiku, S. Diouf, M. Durowoju, I. Ibrahim, et al., Electrical conductivity of Cu and Cu-2vol.% Nb powders and the effect of varying sintering temperatures on their mechanical properties using spark plasma sintering, *Silicon India* (2017) 1–11.
- [49] J.Y. Kim, M.-W. Oh, S. Lee, Y.C. Cho, J.-H. Yoon, G.W. Lee, et al., Abnormal drop in electrical resistivity with impurity doping of single-crystal Ag, *Sci. Rep.* 4 (2014).
- [50] C. Steinborn, M. Herrmann, U. Keitel, A. Schönecker, J. Räthel, D. Rafaja, et al., Correlation between microstructure and electrical resistivity of hexagonal boron nitride ceramics, *J. Eur. Ceram. Soc.* 33 (2013) 1225–1235.
- [51] R. Sule, Synthesis of Copper Tantalum Ruthenium Composites for Electronics Interconnection Applications, 2011.
- [52] D. Kim, S. Hwang, S. Chun, The wetting, reaction and bonding of silicon nitride by Cu–Ti alloys, *J. Mater. Sci.* 26 (1991) 3223–3234.
- [53] S. Wolf, A. Levitt, J. Brown, Whisker–metal Matrix Bonding, *Chemical Engineering Progress*, Amer inst chemical engineers 345 E 47TH ST, New York, NY 10017, 1966, p. 74.
- [54] S. Nagarjuna, M. Srinivas, K. Balasubramanian, D. Sarma, On the variation of mechanical properties with solute content in Cu–Ti alloys, *Mater. Sci. Eng.* 259 (1999) 34–42.
- [55] F. Kustas, Friction and Wear of Titanium Alloys, Friction, lubrication and wear technology, Metals park, 1992.
- [56] M. Long, H. Rack, Titanium alloys in total joint replacement: a materials science perspective, *Biomaterials* 19 (1998) 1621–1639.